Wang−Landau Simulation of Polymer−Nanoparticle Mixtures

Dmytro Antypov and James A. Elliott*

Department of Materials Science and Metallurgy, Pembroke St., Cambridge CB2 3QZ, U.K.

Received June 5, 2008; Revised Manuscript Received July 24, 2008

ABSTRACT: The behavior of a coarse-grained polymer chain in the solution containing two types of interacting species is studied using a face-centered cubic lattice model. The majority component in our model represents the solvent, while the active low volume fraction component is regarded as reversibly adsorbing nanoparticles. Using a novel density-biased method, we calculate the complete phase diagram, which demonstrates the effect of addition of freely moving interactive centers on the equilibrium properties of a polymer chain immersed in either good or poor solvent. Three distinct collapsed and one extended phase are found, each phase comprising two regions with different polymeric degrees of freedom.

I. Introduction

Polymer solutions containing additives ranging from small surfactant molecules to proteins, nanoparticles, and colloids play an important role in a variety of biological systems and industrial applications. These include pharmaceutical and personal care products, paints, surface coatings, and nanocomposite materials. In most cases of naturally occurring biomineralization, the mediators of interactions between nanoparticles are large macromolecules, such as polysaccharides and polypeptides.[1] This idea has also been utilized in laboratory experiments to control crystallization and growth of nanoparticles by using polyelectrolytes, biopolymers, or hydrophilic block copolymers.[2] Water-soluble polymers like poly(ethylene glycol) are often added to protein solutions to induce their crystallization.[3] A number of techniques employing biodegradable polymers are used in the pharmaceutical industry to encapsulate drugs.[4] Polymers are often used in nanofabrication[5] mainly to coat large particles or, more recently, to control the synthesis of small (less than 3 nm in diameter) nanoparticles.[6]

Depending on the relative sizes of the polymer chains and the additives, these systems fall into two different categories. First, a so-called "colloid limit", is where the radius of the particles, R, is much larger than the polymer gyration radius, R_g. In this type of system the nonadsorbing polymer acts as a depletion agent and results in a well-known Asakura−Oosawa type attraction between the large colloidal particles.[7] The polymer−polymer interactions and any changes in the conformational behavior of individual polymer chains are believed to be of secondary importance and are neglected in this and other mean-field theories.[8−10] However, more elaborate theories,[11−17] which take polymeric degrees of freedom into account, and the experimental data (see ref 18 and references therein) indicate that the role of the conformational effects increases as the size of the colloidal particles decreases. These effects become particularly important in the second type of mixture, the so-called "protein limit", when small particles are added to relatively large polymer chains, i.e., $R \ll R_g$.

Much experimental, theoretical, and computational work has been carried out to define how the system parameters are responsible for the phase behavior and physical properties of the polymer−particle mixtures. Whether the mixture remains homogeneous or not depends on the balance between all energetic and entropic effects present in the system. Taking these into account makes theoretical description challenging, especially for the "protein limit".[19] Even in the case of a homogeneous phase, there is always the question of how the additives affect the properties of the mixture.

For some polymer−particle mixtures, the attractive interactions are relatively weak, and the system's behavior is governed primarily by steric repulsions. For example, silica spheres and polystyrene coils suspended in benzene,[20] toluene,[21,22] or cyclohexane[21,23] have a phase diagram typical for an athermal polymer−particle mixture. The system is homogeneous only at low concentrations of the polymer and silica particles. If the content of either component is increased, the mixture can become no longer miscible. The size ratio, $q = R_g/R$, is directly related to the miscibility of the mixture. Since radius of gyration increases with improving solvent properties, higher q values result in better miscibility for better solvents.[21,24] For this same reason, the increase in miscibility can be seen as the temperature of the mixture is increased.[20−22] However, the phase behavior cannot be described in terms of the size ratio q alone. In all the above studies, the miscibility at low particle content indeed improved for longer chains as a function of the reduced polymer concentration, c/c^*, where c^* is the overlap concentration. The same trend was followed by the polymer−particle mixtures in good solvents at higher particle concentrations. Under ideal or Θ solvent conditions, however, this trend was found to be reversed: larger chains cause phase separation at a lower value of c/c^*.[24] Naturally, these observations contradict the predictions of the classical mean-field theories,[7,9] which are built around the q ratio, but are in agreement with the PRISM theory,[21] which takes polymer−polymer interactions into account. Computer simulations of ideal chains and chains with excluded volume qualitatively also agree with the experimental findings and additionally predict different behaviors for critical concentrations in these two idealized cases.[25] Unfortunately, quantitative agreement between the simulations and experiment has not been observed due to the Flory−Huggins χ parameter being considerably higher than zero in the experiments.[23]

The above studies clearly indicate that the solvent quality is an important parameter affecting the phase behavior of the polymer−particle mixtures. It affects both the local effective polymer−polymer interaction and the gyration radius of the coil. What should also be taken into account is that the addition of small particles can affect the equilibrium conformation of the chain, too. When small hard particles are added to a dilute polymer in a good solvent, steric interactions expel them from the polymer coil.[26] This results in a radial concentration gradient of the particles, and the corresponding osmotic pressure acting on the coil always reduces its dimensions.[27,28] Within a mean-field approach, the addition of small particles is equivalent to

* To whom correspondence should be addressed. E-mail: jae1001@cam.ac.uk.

10.1021/ma8012652 CCC: $40.75
Published on Web 09/04/2008

worsening the solvent properties and can be described in terms of the classic Flory−Huggins theory with χ parameter adjusted appropriately according to the particle size and concentration.[12] The reduction of gyration radius in polymer−particle mixtures has been observed experimentally by Kramer and co-workers using small-angle neutron scattering.[29,30]

The effect of additives on polymer conformation in dense polymer−nanoparticle composites is a subject of an ongoing debate.[31−33] The high density of such composites means that the polymer−polymer interactions are not limited only to the intrachain interactions but are actually dominated by the interaction between different chains. On one hand, following Flory's argument, this means that a polymer chain in a dense melt follows the same scaling properties as an ideal chain. On the other hand, the actual gyration radius is difficult to predict. The changes to polymer conformation observed experimentally and in computer simulations appear to be small and, as expected, become more profound as the particle load is increased. Whether these changes are positive,[32−35] negative,[34] or just too small to be registered experimentally[31] depends on the relative size of the additives and their specific interactions with the polymer matrix. All of the above experiments used composite materials prepared via a solvent evaporation technique, which highlights the fact that good dispersion of the nanoparticles in the solution is a prerequisite to obtaining nanocomposite materials with well-controlled physical properties.

While high affinity between polymer and nanoparticles results in swelling of polymer coils in dense nanocomposite materials,[35] addition of attractive particles can result in a chain collapse in a dilute solution.[36−39] This phenomenon can be explained in terms of effective mediated attraction between the monomers and is similar in nature to a polymer collapse in a binary solvent.[40]

In this paper we choose to avoid any polymer or solvent specific interactions and use a simplified model to address generic thermodynamic properties of a polymer chain in a complex environment. For this we employ a lattice model, which has been widely used to describe polymeric systems in both theoretical studies and computer simulations. The thermodynamic properties of interacting self-avoiding random walks (SAWs) give a good qualitative description of the basic balance between entropic and enthalpic terms in experimental polymeric systems. Perhaps the best known example of this is that the coil−globule transition, and its scaling properties are correctly described by the SAWs on a lattice. High coordination lattices like BFM,[41] for example, can also capture the crystallization of a polymer globule at low temperatures.[42]

A number of powerful computational techniques can be used to calculate thermodynamic properties of SAWs at various temperatures in a single computer simulation.[42−46] They all share the idea of sampling different parts of the conformational space uniformly and using the collected information to calculate the partition function and the properties of interest at a given temperature. For example, the multicanonical chain-growth algorithm presented in ref 43 and flatPERM algorithm[44] both bias the chain growth process to equally explore compact and extended conformations. More general methods based on adaptive umbrella sampling technique, like Wang−Landau algorithm[45] for example, encourage the system to visit those energy levels it has explored the least. At the end of the simulation, all energy levels are expected to be visited with similar probabilities, and the free energy profile is calculated as a result. The above methods have been successfully applied to study phase behavior of a free polymer chain[42−44] and a polymer chain adsorbed on a flat surface.[46,47]

In this paper we utilize the Wang−Landau simulation technique to study equilibrium behavior of a free polymer chain in the presence of a large number of small interacting particles. We optimize the calculations by considering only the particles in the immediate vicinity from the chain while the presence of all other particles is taken into account by an appropriate biassing scheme. For mobile particles, we observe conformational behavior qualitatively different from that seen for randomly distributed fixed particles.[48] Our results are in good agreement with the previous simulations of interacting polymer−particle mixtures in a good or Θ solvents[37−39] and additionally cover the poor solvent regime. The computational technique we used does not suffer from sampling difficulties present in the standard Monte Carlo method[39,48] and was able to provide reliable data over a wide range of interaction parameters. For a dilute solution, we obtain the complete phase diagram which includes a number of phases not reported previously.

The remainder of this paper is organized as follows. In section II, we give the details of the model and methodology we use and outline the scope of their applicability. Sections III and IV contain the main results of our study, and their detailed analysis is followed by conclusions in section V.

II. Computational Model and Methodology

Here we adopt a so-called "cell model" approach widely used to study equilibrium properties of macromolecules in dilute solutions.[49,50] In this approach, the polymer concentration, c_p, is assumed to be low enough to neglect correlations between the chains, and a single chain confined to a cell of volume $V = 1/c_p$ is taken to represent such a solution. The number of nanoparticles inside the cell is defined by their bulk concentration, c_n, and is given by $N_n = Vc_n$. The shape of the cell is not uniquely defined—the only purpose of the cell is to impose bulk concentrations c_p and c_n. As a model system we use a face-centered cubic (fcc) lattice—a high coordination regular lattice, where each site has $z = 12$ equidistant closest neighbors. Each site represents one of the three species: polymer (p), nanoparticle (n), or solvent (s). The polymer chain is modeled as a set of N_p connected lattice sites, whereas each nanoparticle occupies a single site.[51] This is equivalent to the assumption that their diameter has a similar magnitude to a polymer Kuhn segment. Multiple occupancy is not allowed, and the interactions between closest neighbors are described by finite square well potentials $E_{\alpha\beta}$, where α and β are any two of $\{p, n, s\}$, giving a total of six unique interaction strengths. However, similar to the Flory−Huggins interaction parameter, defined for a binary mixture as

$$\chi_{\alpha\beta} = \frac{z}{k_B T}\left(E_{\alpha\beta} - \frac{E_{\alpha\alpha} + E_{\beta\beta}}{2}\right) \quad (1)$$

only three independent parameters of form (1) are needed to fully describe the interactions in a ternary lattice system. If we assume that solvent and nanoparticle sites only interact with the polymer, but not with each other (i.e., $E_{nn} = E_{ss} = E_{ns} = 0$), then only two independent parameters remain: i.e., systems having the same combinations of $(E_{pn} - E_{pp}/2)$ and $(E_{ps} - E_{pp}/2)$ will have the same phase behavior.

For the purpose of symmetry and without loss of generality we set $E_{pp} = 0$ and interpret the interactions in terms of E_{pn} and E_{ps}. The partition function can be written

$$Z = \sum D(N_{pn}, N_{ps}) \exp(-\varepsilon_{pn} N_{pn} - \varepsilon_{ps} N_{ps}) \quad (2)$$

where N_{pn} and N_{ps} are respectively the number of polymer−nanoparticle and polymer−solvent closest neighbor pairs and $\varepsilon_{pn} = E_{pn}/(k_B T)$ and $\varepsilon_{ps} = E_{ps}/(k_B T)$ are dimensionless parameters describing the strengths of the corresponding interactions in units of $k_B T$. The sum in eq 2 runs over all possible energy

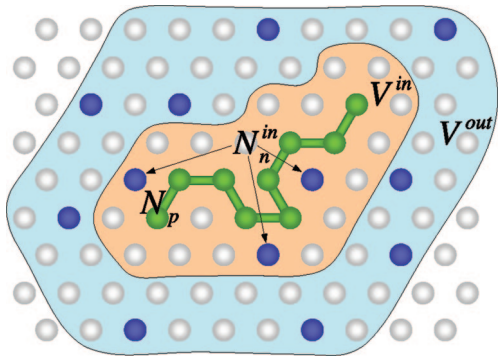

Figure 1. Two-dimensional representation of the polymer−nanoparticle lattice cell model. In this example, $N_n^{in} = 3$ particles can be found within first neighbor shell, $V^{in} = 20$, around the polymer of length $N_p = 9$. Together they form $N_{pn} = 8$ contacts with the polymer, and there are also $N_{ps} = 26$ polymer−solvent contacts in V^{in}. Thus, the pair (N_{pn}, N_{ps}) defines the macrostate to which this microstate belongs.

macrostates, and $D(N_{pn}, N_{ps})$ is the degeneracy of each macrostate. It is convenient to define a density of states matrix $g(N_{pn}, N_{ps}) = D(N_{pn}, N_{ps})/Z$, which gives the probability of observing each macrostate at $1/(k_BT) = 0$. To obtain this matrix, one can take an ensemble of random self-avoiding walks of length N_p and calculate the contribution of each chain conformation to all possible macrostates by placing N_n particles in volume $V - N_p$. Note that only those $N_n^{in} \ll N_n$ particles placed in the immediate neighborhood of the chain, V^{in}, and making N_{pn} polymer−nanoparticle pairs define the resulting macrostate (Figure 1). The remaining $N_n^{out} = N_n - N_n^{in}$ particles placed in remaining $V^{out} = V - N_p - V^{in}$ lattice sites contribute only to the degeneracy factor. This factor, proportional to the probability of having exactly N_n^{in} particles in volume V^{in}, is given by hypergeometric distribution:

$$p = \frac{{}_{V^{in}}C_{N_n^{in}} {}_{V^{out}}C_{N_n^{out}}}{{}_{V-N_p}C_{N_n}} \tag{3}$$

Now, by placing particles only in V^{in} (N_n^{in} can be any number between 0 and V^{in}) the corresponding probabilities of form (3) will give the contribution of the given polymer conformation to the density of states matrix. This approach allows us to reduce calculation load in the computer simulation by considering only the small number of particles in close proximity to the chain. To efficiently sample configurational phase space, we combine this approach, normally used in the grand-canonical ensemble simulations,[52] with Wang−Landau sampling.[45]

The first example we consider here is a polymer chain of length $N_p = 100$ on an fcc lattice of $V = N_p^3$ sites, 10% of which are occupied by nanoparticles. This choice of system parameters means that the solvent is the majority component of the system and that the chain is long enough to clearly observe changes in its conformation. For each of $\sim 3.5 \times 10^{99}$ possible chain conformations there are ${}_{10^6}C_{10^5} \approx 10^{10^5}$ possible arrangements of particles in the box. This enormous number of microstates is grouped into just over 2×10^5 different macrostates defined by all possible pairs (N_{pn}, N_{ps}). To generate a new polymer conformation, a cooperative move preserving chain connectivity was employed.[53] The polymer move was alternated with a random exchange of a nanoparticle between V^{in} and V^{out}. The new state was accepted with probability

$$p(1 \rightarrow 2) = \min\left[\frac{g(1)p(2)}{g(2)p(1)}, 1\right] \tag{4}$$

where 1 and 2 denote the old and the new state of the system and p is given by eq 3for each state. When a polymer bead is moved, extra care has to be taken of those lattice sites which did not belong to V^{in} previously. First, with a probability of N_n^{out}/V^{out}, particles are placed in each of these sites to mimic the presence of N_n^{out} particles in V^{out} and to preserve the detailed balance condition for this move. Then, the new state is accepted with the probability given by eq 4, and the corresponding element of the density of states matrix $g(N_{pn}, N_{ps})$ is multiplied by modification factor f.[45] Once all macrostates have been visited an approximately equal number of times (i.e., a flat energy histogram has been achieved), the modification factor is reduced according to the $f_{i+1} = \sqrt{f_i}$ rule. We found that $\sim 2 \times 10^7$ MC trials per macrostate and a final modification factor of 1.000 000 1 were sufficient for good convergence. This single processor calculation took 3 weeks on a conventional desktop computer, and an analogous simulation was run at a fixed density of states matrix to calculate the observables.

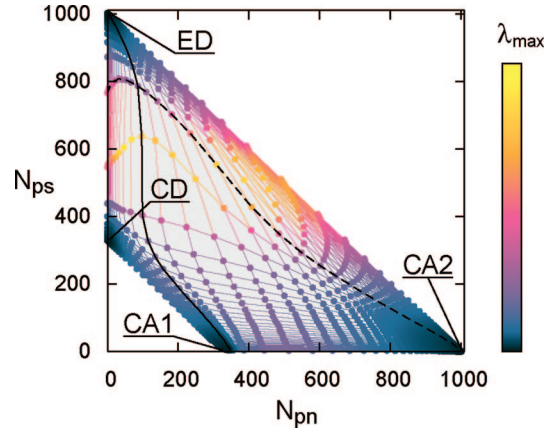

Figure 2. Each point on the gray background corresponds to the position of the free energy minimum at given combination of the interaction parameters, $-4 \le \varepsilon_{pn} \le 4$ and $-4 \le \varepsilon_{ps} \le 4$ with a grid step of 0.1, represented in the space of number of polymer−solvent (N_{ps}) and polymer−nanoparticle (N_{pn}) contacts. The white areas of the diagram are forbidden due to the spatial constraints. Higher values of λ_{max} separate four phases located in each corner of the diagram: extended desorbed (ED), collapsed desorbed (CD), and two different collapsed adsorbed phases (CA1 and CA2).

We also performed an explicit simulation of the polymer chain together with all N_n particles in volume V and found two apparent advantages of using the density-biased method with fewer particles. First, the calculation time reduces significantly, resulting in an ~ 2 orders of magnitude speed-up for the above parameters. Second, since V is only a parameter in the acceptance criterion (4) but not the actual volume of the simulation box, polymer concentrations higher than N_p^{-3} can be studied without the chain starting to interact with its periodic image.

III. Results: Phase Diagram

Definition of Phases. In this section, we analyze the phase diagram of a polymer solution characterized by chain length $N_p = 100$ and polymer concentration $c_p = 1/N_p^3$ in the presence of interacting particles at 10% volume fraction. Knowledge of the density of states matrix allows us to calculate the system's free energy and specific heat for any given pair of interaction strengths $(\varepsilon_{pn}, \varepsilon_{ps})$. For $-4 \le \varepsilon_{pn} \le 4$ and $-4 \le \varepsilon_{ps} \le 4$, we explored the free energy minimum landscape and found that for any combination of $(\varepsilon_{pn}, \varepsilon_{ps})$ there was only one minimum. This contrasts with the chain adsorption on a surface, for which layering states separated by free energy barriers are observed.[47,46] The number of polymer−nanoparticle (N_{pn}) and polymer−solvent (N_{ps}) contacts at the most probable state are depicted in Figure 2 for a discrete set of $(\varepsilon_{pn}, \varepsilon_{ps})$, with grid increments of 0.1. For this model chain,

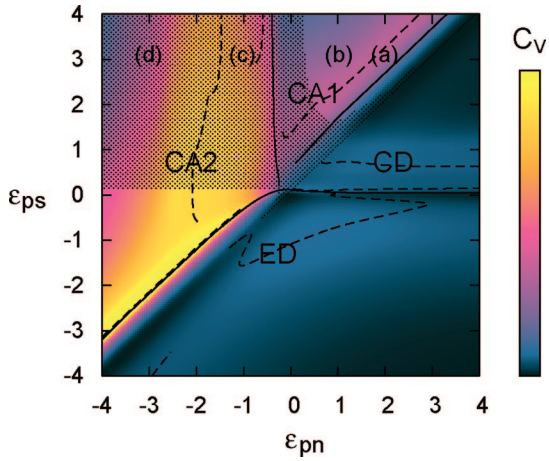

Figure 3. (ε_{pn}, ε_{ps}) pseudophase diagram color coded according to the specific heat C_V. The solid lines indicate positions of λ_{max}, whereas the dashed lines mark peaks in C_V. The dotted area indicates where addition of nanoparticles causes the polymer chain to swell. Typical collapsed conformations at $\varepsilon_{pn} = 3$ and (a) $\varepsilon_{ps} = 2$, (b) $\varepsilon_{ps} = 1$, (c) $\varepsilon_{ps} = -1$, and (d) $\varepsilon_{ps} = -3$ are shown in the Supporting Information and described in detail in the text.

there are $N_p(z-2)+2 = 1002$ possible polymer contacts which are split between the intrachain contacts and the contacts with the solvent and particles. At extremely strong attractions, the chain is completely covered by the nanoparticles (bottom right corner) or the solvent (upper left corner). The lines coming from the upper left corner correspond to constant ε_{pn}, and the solvent properties worsen as we follow the line down (the black solid line illustrates $\varepsilon_{pn} = 0$). Similarly, all lines crossing in the bottom right corner of the diagram correspond to a fixed polymer−solvent interaction ε_{ps} which increases as we move to the left (the black dashed line illustrates $\varepsilon_{ps} = 0$). The colors in Figure 2 denote the magnitudes of the largest eigenvalue, λ_{max}, of the matrix of second derivatives of the free energy with respect to ε_{pn} and ε_{ps}. This quantity shows how rapidly the system's entropy changes upon variation of the interaction strengths and was previously used to locate phase boundaries for the polymer adsorption near a wall.[47] A locus of points with high λ_{max}, indicative of a phase boundary, clearly separates the top and the bottom parts of the diagram. The radius of gyration (see Supporting Information) indicates that the top of the diagram in Figure 2 corresponds to extended coil conformations, whereas the polymer chain is collapsed in the bottom part of the diagram. There are three distinct types of collapsed phases separated by higher values of λ_{max}: a collapsed desorbed (CD) phase at $N_{pn} = 0$ and two distinct collapsed adsorbed phases (CA1 and CA2) at $N_{ps} = 0$.

Figure 3 shows these four phases separated by sharp changes in the system's entropy in (ε_{pn}, ε_{ps}) plane. The color coding this time shows the specific heat calculated as energy variation with temperature at fixed interaction strengths (E_{pn}, E_{ps}). Note that this corresponds to a straight line passing through the origin of Figure 3 for each ratio (E_{ps}/E_{pn}) is fixed. The difference between the positions of solid and dashed lines in Figure 3 arises from different signatures and the ambiguity of defining phase transitions in a finite system. In general, the position of the phase boundaries are chain length dependent and, for lattice systems, can also merge in the thermodynamic limit.[42]

Pure Solvent. To understand complex behavior in Figure 3, let us first consider a chain in a pure solvent. This corresponds to the diagonal line ($\varepsilon_{ps} = \varepsilon_{pn}$) where nanoparticles are essentially indistinguishable from the lattice sites representing solvent. At the top right corner of the diagram, strong repulsion between the polymer and bulk lattice sites results in a compact

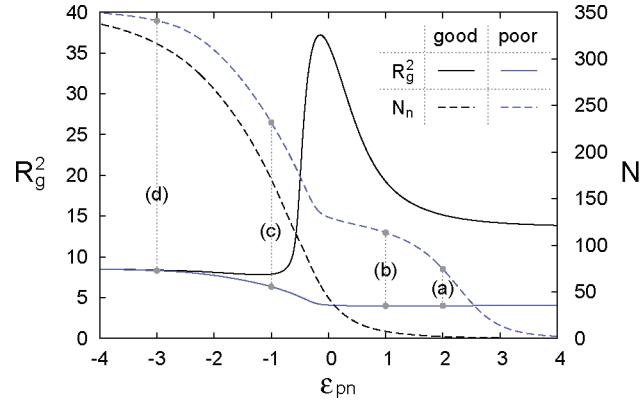

Figure 4. Mean-square gyration radius R_g^2 and number of adsorbed particles N_n as a function of ε_{pn} under good solvent ($\varepsilon_{ps} = 0$) and poor solvent ($\varepsilon_{ps} = 3$) conditions. Four adsorption regimes in poor solvent are (a) crystallized polymer, (b) surface adsorbed globule, (c) volume adsorbed globule, and (d) swollen globule. Typical collapsed conformations are shown in the Supporting Information and described in detail in the text.

crystalline structure. As the interaction is decreased, the chain adopts a droplet-like globular conformation at about $\varepsilon_{pn} = \varepsilon_{ps} = 0.80$. At $\varepsilon_{pn} = \varepsilon_{ps} = 0.13$ the chain undergoes a globule−coil transition and remains in an extended state as the interaction decreases. A peak in specific heat at $\varepsilon_{pn} = \varepsilon_{ps} = -0.85$ indicates transition between a random coil and a coil that is stiffened and stretched due to association with the attractive solvent.

Poor Solvent. The effect of nanoparticles on polymer behavior under poor solvent conditions can be clearly traced at relatively high positive values of ε_{ps}. At $\varepsilon_{ps} = 3$, the presence of repulsive particles only weakly affects the very compact crystal-like conformation. There is no preferable absorption of nanoparticles at $\varepsilon_{pn} = \varepsilon_{ps} = 3$. If we decrease ε_{pn} at constant ε_{ps} and cross the boundary between CD and CA1 phases, the nanoparticles wet the surface of the crystalline globule (Figures 3 and 4, point (a)). As ε_{pn} is decreased further, the crystalline structure melts (dashed line in CA1), slightly increasing the globule surface to volume ratio and adsorbing more nanoparticles (Figures 3 and 4, point (b)). It is still improbable for a nanoparticle to be found inside the polymer globule, and adsorption takes place only on its surface. As we cross the boundary between CA1 and CA2, the polymer−nanoparticle attraction drives particles inside the globule (Figures 3 and 4, point (c)). The number of adsorbed particles increases, many of them having multiple contacts with polymer beads (only in this phase is it likely to find a nanoparticle with all 12 nearest-neighbor lattice sites occupied by the polymer). The chain conformation remains compact but swells slightly as more particles are adsorbed at even lower ε_{pn} (Figures 3 and 4, point (d)).

Good Solvent. If we similarly vary polymer−nanoparticle interaction along line $\varepsilon_{ps} = 0$, this will correspond to good solvent conditions. Starting again from high values of ε_{pn}, we find that repelling particles (note that these can be viewed as hard larger particles occupying 13 lattice sites) decrease chain dimensions (Figure 4). Figure 4 also shows that addition of weakly adsorbed particles ($\varepsilon_{pn} < 0$) to a polymer in good solvent results in a small increase of the gyration radius. However, as ε_{pn} is decreased, the coil collapses into the structure similar to that observed in poor solvent at point (c). At $\varepsilon_{pn} \approx -1.18$, the chain has the most compact conformation which swells slightly at lower ε_{pn} as more particles are adsorbed.

Effect of Particle Mobility. The above behavior contrasts with the chain adsorption in the media of fixed randomly distributed particles, where the radius of gyration significantly

increases at high adsorption strengths.[48] From the statistical mechanics point of view this is rather surprising since the partition function is not affected by the particle mobility. Hence, the results must be identical provided each system is ergodic and can explore all possible conformations. This is the case at low attraction strengths, where our results agree with those presented in ref 48; i.e., the initial increase in R_g is followed by a chain collapse as the attraction strength is increased. In the medium of fixed particles, this means that the chain spends more time in the areas with high local concentration of particles and on average samples the same conformational space as a chain surrounded by mobile particles. However, there are two reasons why the chain behavior in the medium of fixed particles starts to deviate at higher adsorption strengths. First, a thermodynamically more favorable collapsed state corresponds to a relatively high localization of particles, and such density fluctuation is unlikely to be found in a relatively small simulation box of fixed random particles. Second, the chain mobility decreases sharply at higher adsorption strengths, and it is not able to diffuse to find the appropriate particle neighborhood. As a result, the polymer chain becomes trapped between the fixed particles at relatively low concentration. Consequently, this glassy state, observed in ref 48, is characterized by much higher chain dimensions when compared to the thermodynamically more favorable collapsed state.

Chain Dimensions. The chain dimensions were compared to those under pure solvent conditions, i.e., when nanoparticles and solvent sites are indistinguishable ($\varepsilon_{ps} = \varepsilon_{pn}$). The area where the chain swells in the presence of nanoparticles is marked by dots in Figure 3. For the chain to swell, the particles have to have a higher affinity for the polymer than the solvent. This window is very narrow in the ED phase, while the polymer globule in a poor solvent tends to swell by adsorbing particles. There is a clear region in phase CA1 where the radius of gyration is some 1% lower than its value on the diagonal $\varepsilon_{ps} = \varepsilon_{pn}$. This is purely a finite size effect due to the fact that the most compact conformation of the chain is not perfectly spherical. For repulsive particles below the diagonal $\varepsilon_{ps} = \varepsilon_{pn}$ in the CD phase, the difference is analogously small. Note also that particle adsorption destabilizes crystal structure in phase CA1 when compared to phase CD in which repelling particles do not affect polymer conformation (the dashed line in phase CD is nearly horizontal). Here the crystal-like structure melts when ε_{ps} is decreased. The dashed line in phase ED defines the transition between a random coil and a coil stiffened and stretched due to adsorption of the solvent onto the polymer.

IV. Results: Effect of Particle Concentration and Chain Length

Two additional simulations were performed to assess the effect of the system parameters. First, a polymer chain of the same length of $N_p = 100$ was studied in the solution with the particle content reduced to 5%. Second, a longer chain of $N_p = 200$ was simulated at 10% of particles.

Effect of Particle Concentration. The phase behavior of the 5% and the 10% systems was found very similar. Taking into account the symmetry of the model, the particle sites and solvent sites become identical when $\varepsilon_{ps} = \varepsilon_{pn}$. Therefore, all transition lines close to the diagonal only weakly depend on the particle concentration. Away from this diagonal, however, there was a small but marked shift of all phase boundaries toward higher interaction strengths. For example, the melting of the polymer globule in a poor solvent (dashed line in phase CA1 in Figure 3) occurs due to the adsorption of particles on its surface and the subsequent screening of the poor solvent. Therefore, a stronger polymer−particle interaction is required to adsorb

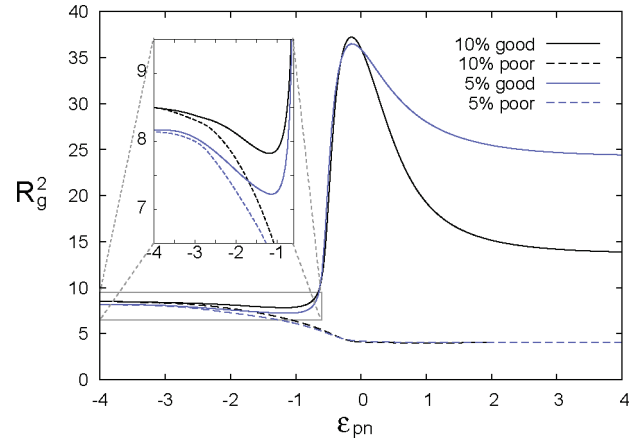

Figure 5. Mean-square gyration radius R_g^2 as a function of polymer−particle interaction strength ε_{pn} under good solvent ($\varepsilon_{ps} = 0$) and poor solvent ($\varepsilon_{ps} = 3$) conditions calculated at 10% and 5% of particle content.

enough particles from a more diluted solution to cover the globule surface.

The effect of particle concentration on the equilibrium polymer conformation is summarized in Figure 5. Under good solvent conditions the addition of small repulsive particles ($\varepsilon_{pn} > 0$) results in the reduction of the polymer coil dimensions—a higher particle concentration produces a bigger reduction. The addition of weakly attractive particles ($-0.14 < \varepsilon_{pn} < 0$) increases the polymer coil dimensions—the higher the particle content, the steeper this increase. However, as the polymer−particle attraction is increased further, the polymer chain experiences a collapse. The inset in Figure 5 shows that at lower particle content the chain adopts a more compact conformation at similar value of $\varepsilon_{pn} \approx 1.18$. At strong polymer−particle attraction, the chain swells by adsorbing more particles from the solution. The size of this "swollen globule" conformation depends only on the particle concentration but not on the solvent properties. Under both good and poor solvent conditions the system adopts the same conformation, whose size decreases as the particle concentration decreases.

At fixed ε_{ps} and ε_{pn} the number of particles adsorbed onto the polymer chain was found to be always higher in the 10% system. Even if there was no attraction between the polymer and the particles (i.e., $\varepsilon_{pn} = 0$), some particles are still found in close proximity to the polymer. Figure 6 demonstrates this phenomenon for both 5% and 10% systems as a function of solvent properties. Under good solvent conditions, $\varepsilon_{ps} = 0$, the average number of sites available in the vicinity of the chain of length $N_p = 100$ is approximately $V^{in} \approx 434.7$. Correspondingly, 5% or 10% of these sites are taken by particle sites at $\varepsilon_{pn} = 0$. For $\varepsilon_{ps} < 0$, the solvent sites are attracted to the polymer and displace the particle sites from V^{in} (as a result, the polymer coil swells slightly and V^{in} increases). As the solvent properties worsen at $\varepsilon_{ps} > 0$, the polymer coil dimensions reduce, correspondingly reducing the surface area exposed to both the solvent and the particles. As the polymer collapses to a compact globule, the neutral particles reside near its surface screening the polymer from highly repellent solvent. There are no particles inside the globule (surface adsorption, phase CA1 in Figure 3), and their number on the surface becomes a weak function of particle concentration as particles completely cover the polymer globule.

The collapse scenario is completely different in the case of adsorbing particles with $\varepsilon_{ps} = -1$. These particles trigger polymer collapse even in a good solvent, resulting in a "volume adsorbed" conformation (phase CA2 in Figure 3). Here the effect of the solvent is secondary—the polymer collapse is a way of

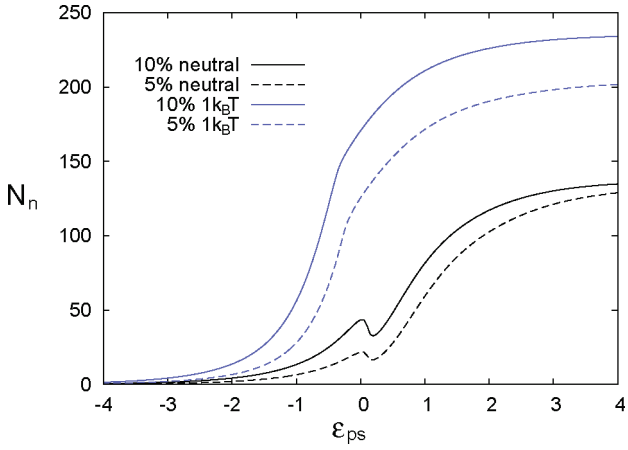

Figure 6. Number of adsorbed particles N_n as a function of solvent quality ε_{ps} ($\varepsilon_{ps} = 0$ corresponds to athermal or good solvent conditions, positive values of ε_{ps} correspond to poor solvent conditions, and negative ε_{ps} represent the situation of strong polymer−solvent attraction). The data are shown for both neutral particles with $\varepsilon_{pn} = 0$ and attractive particles with $\varepsilon_{pn} = -1$.

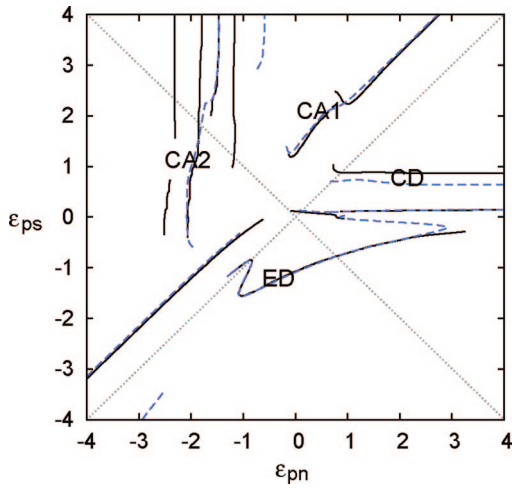

Figure 7. Positions of peaks in specific heat in (ε_{pn}, ε_{ps}) plane calculated for a chain of $N_p = 200$ (solid lines) and a chain of $N_p = 100$ dashed lines. Dotted lines show diagonals $\varepsilon_{ps} = \varepsilon_{pn}$ and $\varepsilon_{ps} = -\varepsilon_{pn}$ to guide the eye.

decreasing the system free energy by increasing the number of polymer−particle contacts N_{pn} at the expense of the conformational entropy of the polymer and translational entropy of the particles. Because each adsorbed particle bears an entropy penalty (the lower the particle concentration, the higher this penalty), the number of particles adsorbed by the globule is lower at lower particle contents. This is also reflected by the size of the globule at low values of ε_{pn} in inset of Figure 5.

Effect of Chain Length. To see how the phase boundaries change as the chain length increases, we simulated a chain of length $N_p = 200$ suspended in a solution containing 10% of nanoparticles. Figure 7 shows the positions of calculated maxima in specific heat for this system. The same lines as calculated for a shorter chain of $N_p = 100$ and shown in Figure 3 are also given in Figure 7 for comparison. The first difference between these two systems which can be noticed is a number of nearly vertical lines in the CA2 phase. A closer analysis, however, shows that these small local peaks in specific heat are model artifacts and originate from the discrete nature of the fcc lattice. For a fixed set of polymer−solvent and polymer−nanoparticle interactions the specific heat profile as a function of temperature has a nearly horizontal plateau within the CA2 phase. For example, for a line $\varepsilon_{ps} = -\varepsilon_{pn}$ the specific heat of a collapsed chain increases sharply up to $\varepsilon_{pn} \approx -1.0$ and then reaches a horizontal plateau before decreasing rapidly at $\varepsilon_{pn} \approx -2.4$. The color coding in Figure 3 shows a similar flat region in the specific heat for $N_p = 100$. A number of ripples on this plateau result in the distinct maxima seen in Figure 7. The position of the absolute maxima, however, correlates well with the dashed line calculated for $N_p = 100$. Also, when normalized by the chain length, the specific heat profiles in the CA2 phase are very similar for both chain lengths. Therefore, the transition between a compact volume-adsorbed globule and a swollen globule is characterized by local rearrangement of the particles within the globule and does not depend on the chain length. However, if the particle concentration is changed, the position of this transition also changes: at higher particle concentrations, the swollen globule behavior onsets at a weaker polymer−nanoparticle attraction.

If we follow the line $\varepsilon_{ps} = -\varepsilon_{pn}$ in Figure 3 to the ED phase, the chain surroundings change to the opposite: there are 10% of repulsive and 90% of attractive sites. Here again we find that the phase boundaries between the random coil and the stretched coil are the same for both chain lengths. The specific heat profiles normalized by the chain length are practically identical, which indicates that this transition (which is a chain expansion in an attractive solvent) is also local in nature. It is related to the loss of chain flexibility due to the solvent and is not a lattice artifact. In our off-lattice simulations of a polymer in an attractive solvent (to be published elsewhere) we found that the specific heat is also a nonmonotonic function of temperature with a maximum at ε_{ps} of order of several k_BT. The similarities between the CA2 and ED phases are not surprising since in a symmetric mixture containing 50% of solvent and 50% of particles these two phases become identical. The reason why one phase is collapsed and the other is extended is entirely due to the relatively low content of the nanoparticles in the examples considered here.

Thermodynamic Limit. The boundary between surface adsorbed CA1 and volume adsorbed CA2 phases is expected to remain in the thermodynamic limit. It will separate the area of the phase diagram where particles cannot diffuse through the solvent−polymer interface from the area where they can (driven by the relatively strong attraction to the polymer in phase CA2). However, the melting transition within phase CA1 is affected by the globule's surface-to-volume ratio and is expected to disappear in the thermodynamic limit. The transition within collapsed desorbed phase CD is analogous to polymer crystallization in pure solvent and is expected to have the same behavior in the thermodynamic limit. Despite earlier evidence that in a lattice model this transition is expected to merge with the coil−globule transition,[42] more recent simulations indicate that SAWs on fcc lattice have two separate transition points.[54] The boundaries of the extended phase ED are only weakly affected by the chain length, and both scenarios of the collapse into pure polymer (phase CD) or polymer−particle mixture (phase CA2) should be possible in the thermodynamic limit.

V. Conclusions

A novel method was developed to study a lattice-based polymeric system also containing two types of interacting sites, with the lower volume fraction species representing nanoparticles and the majority species representing solvent. We calculated the free energy and a number of related properties for a single polymer chain over a wide range of interaction strengths to determine the system's phase behavior. Addition of particles with slightly higher than solvent affinity for the polymer resulted in coil swelling within a narrow window of interaction parameters. If the difference

in affinity was large, localization of attractive interactions led to a collapse of a polymer chain, even in good solvent. Because of a high entropic penalty, there was no extended adsorbed phase, and strong adsorption of nanoparticles always led to a collapse of the polymer chain. However, if such particles were added to a collapsed polymer globule in a poor solvent, the globule either adsorbed them on its surface (phase CA1 or "surface adsorption" regime) or swelled by adsorbing them from the solution (phase CA2 or "volume adsorption" regime). Surface adsorption occurs only in a poor solvent, whereas volume adsorption, driven by strong polymer−particle attraction, can take place under any solvent conditions. When adsorption is taking place on the surface of the globule, its dimensions are only very weakly affected by the particle concentration. In contrast, in the volume adsorption regime, the globule size increases with the increasing bulk concentration of nanoparticles. The number of nanoparticles adsorbed this way in the limit of very strong polymer−particle attractions (i.e., the swollen globule part of the CA2 phase) was found to be independent of the solvent properties.

To locate phase boundaries, we calculated the largest eigenvalue, λ_{max}, of the matrix of second derivatives of the free energy with respect to the interaction strengths ε_{pn} and ε_{ps}. High values of λ_{max}, which mean steep changes in system's entropy, indicated the existence of four distinct phases. Our analysis suggests that these four phases will remain in the thermodynamic limit. Additionally, each phase was found to be separated by maxima in heat capacity into two regions corresponding to different polymer degrees of freedom. In the CA1 phase and collapsed desorbed phase CD, this was the difference between globular and crystalline state of the polymer chain, while in CA2 phase and extended desorbed phase ED it was a transition between the random coil conformation and correspondingly a swollen or stretched conformation due to the association of the attractive component. The latter two transitions are similar in nature and originate from the saturated attractive interactions leading to conformational frustration of the polymer chain. In case of the attractive component being in minority, the chain is collapsed, whereas it increases its radius of gyration if the attractive component is abundant. These two transitions are accompanied by broad peaks in the heat capacity whose position and profile do not change with the chain length, hence indicating their local nature. This also indicates that these two transitions will remain in the thermodynamic limit. The crystallization transition in phase CD is also expected to remain a separate transition in the thermodynamic limit, similar to the crystallization transition for interacting SAWs in an fcc lattice.[54] On the contrary, the crystallization transition in phase CA1 is expected to become identical to the transition between phases CA1 and CA2.

We hope our results will contribute to research on phase transitions in finite systems and can be used to map behavior of experimental mixtures. When mapping a particular polymer solution onto the phase diagram, shown in Figure 3, the difference in entropy of a single particle and a given amount of solvent of the same volume is expected to change the positions of phase boundaries, while preserving the qualitative picture. Our results can also be useful to interpret phase diagrams of polymers in mixed solvents.[55] With the incorporation of long-range interactions, it is possible to study polyelectrolyte collapse.[56,57] A detailed description of how to apply the Wang−Landau sampling method to a lattice-based polyelectrolyte was published recently.[58] The preliminary results of ref 58 confirm that the collapse of long chains occurs via a number of intermediate phases. However, it is not clear what these phases are, and a more detailed analysis of the collapsed phase is required.

Acknowledgment. We thank A. Windle for useful discussions and acknowledge financial support from EPSRC Materials Modelling Initiative within the research consortium "Modelling of the Biological Interface with Materials".

Supporting Information Available: Polymer radius of gyration corresponding to Figure 2 and the snapshots of collapsed phases (a), (b), (c), and (d) noted in Figures 2−4. This material is available free of charge via the Internet at http://pubs.acs.org.

References and Notes

(1) Cölfen, H.; Mann, S. *Angew. Chem., Int. Ed.* **2003**, *42*, 2350–2365.
(2) Yu, S.-H.; Cölfen, H. *J. Mater. Chem.* **2004**, *14*, 2124–2147.
(3) McPherson, A. *Methods* **2004**, *34*, 254–265.
(4) des Rieux, A.; Fievez, V.; Garinot, M.; Schneider, Y.-J.; Prat, V. *J. Controlled Release* **2006**, *116*, 1–27.
(5) Hamley, I. W. *Nanotechnology* **2003**, *14*, R39–R54.
(6) Sardar, R.; Park, J.; Shumaker-Parry, J. *Langmuir* **2007**, *23*, 11883–11889.
(7) Asakura, S.; Oosawa, F. *J. Chem. Phys.* **1954**, *22*, 1255.
(8) Gast, A.; Hall, C.; Russel, W. *J. Colloid Interface Sci.* **1983**, *96*, 251.
(9) Lekkerkerker, H.; Poon, W.; Pusey, P.; Stroobants, A.; Warren, P. *Europhys. Lett.* **1992**, *20*, 559–564.
(10) Warren, P. B.; Illet, S. B.; Poon, W. *Phys. Rev. E* **1995**, *52*, 5205.
(11) Aarts, D.; Tuinier, R.; Lekkerkerker, H. *J. Phys.: Condens. Matter* **2002**, *14*, 7551–7561.
(12) Sear, R. P. *Phys. Rev. E* **2002**, *66*, 051401.
(13) Fuchs, M.; Schweizer, K. S. *J. Phys.: Condens. Matter* **2002**, *14*, R239.
(14) Patel, N.; Egorov, S. A. *J. Chem. Phys.* **2005**, *123*, 144916.
(15) Quant, C. A.; Meredith, J. C. *Macromolecules* **2005**, *38*, 167–173.
(16) Surve, M.; Pryamistyn, V.; Ganesan, V. *Langmuir* **2006**, *22*, 969–981.
(17) Hooper, J. B.; Schweizer, K. S. *Macromolecules* **2006**, *39*, 5133–5142.
(18) Mutch, K. J.; van Duijneveldt, J. S.; Eastoe, J. *Soft Matter* **2007**, *3*, 155–167.
(19) Chen, Y.-L.; Schweizer, K. S.; Fuchs, M. *J. Chem. Phys.* **2003**, *118*, 3880.
(20) Vliegenthart, G. A.; van Duijneveldt, J. S.; Vincent, B. *Faraday Discuss* **2003**, *123*, 65–74.
(21) Ramakrishnan, S.; Fuchs, M.; Schweizer, K. S.; Zukoski, C. F. *J. Chem. Phys.* **2002**, *116*, 2201–2212.
(22) Hennequin, Y.; Evens, M.; Angulo, C. M. Q.; van Duijneveldt, J. S. *J. Chem. Phys.* **2005**, *123*, 054906.
(23) Zhang, Z.; van Duijneveldt, J. S. *Langmuir* **2006**, *22*, 63–66.
(24) Shah, S. A.; Chen, Y. L.; Schweizer, K. S.; Zukoski, C. F. *J. Chem. Phys.* **2003**, *118*, 3350–3361.
(25) Bolhuis, P. G.; Meijer, E. J.; Louis, A. A. *Phys. Rev. Lett.* **2003**, *90*, 068304.
(26) Nowicki, W. *Macromolecules* **2002**, *35*, 1424–1436.
(27) van der Schoot, P. *Macromolecules* **1998**, *31*, 4635.
(28) Taylor, M. P. *J. Chem. Phys.* **2004**, *121*, 10757–10765.
(29) Kramer, T.; Schweins, R.; Huber, K. *Macromolecules* **2005**, *38*, 9783–9793.
(30) Kramer, T.; Schweins, R.; Huber, K. *J. Chem. Phys.* **2005**, *123*, 014903.
(31) Sen, S.; Xie, Y.; Kumar, S.; Yang, H.; Bansal, A.; Ho, D.; Hall, L.; Hooper, J.; Schweizer, K. *Phys. Rev. Lett.* **2007**, *98*, 128302.
(32) Tuteja, A.; Duxbury, P.; Mackay, M. *Phys. Rev. Lett.* **2008**, *100*, 077801.
(33) Allegra, G.; Raos, G.; Vacatello, M. *Prog. Polym. Sci.* **2008**, *33*, 683.
(34) Nakatani, A.; Chen, W.; Schmidt, R.; Gordon, G.; Han, C. *Polymer* **2001**, *42*, 3713–3722.
(35) Mackay, M.; Tuteja, A.; Duxbury, P.; Hawker, C.; Horn, B. V.; Guan, Z.; Chen, G.; Krishnan, R. S. *Science* **2006**, *311*, 1740.
(36) Khalatur, P.; Zherenkova, L.; Khokhlov, A. *J. Phys. II* **1997**, *7*, 543–582.
(37) Zherenkova, L.; Mologin, D.; Khalatur, P.; Khokhlov, A. *Colloid Polym. Sci.* **1998**, *276*, 753–768.
(38) Diamant, H.; Andelman, D. *Macromolecules* **2000**, *33*, 8050–8061.
(39) Chodanowski, P.; Stoll, S. *Colloid Polym. Sci.* **2000**, *278*, 406–417.
(40) de Gennes, P. *J. Phys., Lett.* **1976**, *37*, 59–61.
(41) Deutsch, H. P.; Binder, K. *J. Chem. Phys.* **1991**, *94*, 2294.
(42) Rampf, F.; Paul, W.; Binder, K. *Europhys. Lett.* **2005**, *70*, 628–634.
(43) Bachmann, M.; Janke, W. *Phys. Rev. Lett.* **2003**, *91*, 208105.
(44) Krawczyk, J.; Prellberg, T. *Phys. Rev. Lett.* **2004**, *92*, 120602.

(45) Wang, F.; Landau, D. P. *Phys. Rev. Lett.* **2001**, *86*, 2050.
(46) Bachmann, M.; Janke, W. *Phys. Rev. Lett.* **2005**, *95*, 058102.
(47) Krawczyk, J.; Owczarek, A. L.; Prellberg, T.; Rechnitzer, A. *Europhys. Lett.* **2005**, *70*, 726–732.
(48) Huang, J. H.; Mao, Z. F.; Qian, C. J. *Polymer* **2006**, *47*, 2928–2932.
(49) Flory, P.; Orwoll, R.; Vrij, A. *J. Am. Chem. Soc.* **1964**, *86*, 3507–3514.
(50) Deserno, M.; von Grunberg, H.-H. *Phys. Rev. E* **2002**, *66*, 011401.
(51) There is no excluded volume correlation between the positions of single sites on a lattice. It is possible to include the excluded volume interactions between the particles by making them bigger and allowing each particle to occupy several lattice sites. This also means that the correlation zone around the polymer chain has to be increased to a distance at which the particle−particle correlations can be neglected.
(52) Frenkel, D.; Smit, B. *Understanding Molecular Simulation: From Algorithms to Applications*; Academic Press: London, 2002.
(53) Haire, K. R.; Carver, T. J.; Windle, A. H. *Comput. Theor. Polym. Sci.* **2001**, *11*, 17–28.
(54) Vogel, T.; Bachmann, M.; Janke, W. *Phys. Rev. E* **2007**, *76*, 061803.
(55) Termonia, Y. *J. Polym. Sci., Part B: Polym. Phys.* **1999**, *37*, 2782–2787.
(56) Orkoulas, G.; Kumar, S. K.; Panagiotopoulos, A. Z. *Phys. Rev. Lett.* **2003**, *90*, 048303.
(57) Klos, J.; Pakula, T. *J. Chem. Phys.* **2004**, *120*, 2496–2501.
(58) Volkov, N.; Vorontsov-Velyaminov, P.; Lyubartsev, A. *Phys. Rev. E* **2007**, *75*, 016705.

MA8012652